Tropical Journal of Drug Research May 2025; 2 (5):130 - 145
ISSN: 2476-8065 (Electronic)
Available online at http://www.tjdr.org
https://doi.org/10.26538/tjdr/v2i5.2

Original Research Article

Unveiling the Antidiabetic and Anti-Inflammatory Potential of *Piliostigma thonningii* Ethanol Leaf Extract as a Dual PPAR-γ and COX-2 Modulator via In Vitro and Molecular Docking Insights

Mutiu A. Alabi*, Nabilat T. Yakub, Miracle M. Abiola and Emmanuel O. Ajani

Biochemistry Department, Faculty of Pure and Applied Sciences, Kwara State University, Malete 241103, Nigeria

*For correspondence: Email: : mutiu.alabi@kwasu.edu.ng ; +234-7030428661

Sent for review: 19 May 2025 Revised accepted: 31 May 2025

Abstract

Purpose: Diabetes mellitus remains a global health challenge, prompting the search for safer, more effective therapies. *Piliostigma thonningii*, a medicinal plant used in traditional medicine, is known for its antidiabetic and anti-inflammatory properties. This study evaluates the ethanol leaf extract of *P. thonningii* for these activities
Methods: Ethanol leaf extract was analyzed via GC-MS and subjected to in vitro assays. Identified phytochemicals were further assessed using molecular docking.
Results: The extract demonstrated a dose-dependent inhibition of α-amylase and α-glucosidase activities, with IC_{50} values of 68.50 ± 1.84 and 483.70 ± 2.69 µg/ml, respectively, suggesting its potential to regulate postprandial hyperglycemia. Additionally, the extract enhanced glucose uptake and adsorption, reinforcing its hypoglycemic activity. The anti-inflammatory assays revealed significant inhibition of protein denaturation (IC_{50} = 61.50 ± 1.79 µg/ml), proteinase activity (IC_{50} = 63.30 ± 1.80 µg/ml), membrane stabilization (IC_{50} = 58.37 ± 1.77 µg/ml), and heat-induced hemolysis (IC_{50} = 83.97 ± 1.92 µg/ml), indicating its potential as an anti-inflammatory agent. Molecular docking analyses further validated the pharmacological potential of *P. thonningii*, revealing strong binding affinities of its phytochemicals to peroxisome proliferator-activated receptor gamma (PPAR-γ) and cyclooxygenase-2 (COX-2). Notably, anthracene, 1,2,3,4-tetrahydro-9,10-dimethyl- exhibited the highest binding affinity for PPAR-γ (-7.24 kcal/mol), surpassing pioglitazone (-5.64 kcal/mol), while tetratriacontyl trifluoroacetate showed a strong interaction with COX-2 (-6.40 kcal/mol), comparable to celecoxib (-7.13 kcal/mol).
Conclusion: *P. thonningii* exhibits dual antidiabetic and anti-inflammatory potential, supporting its traditional use. Further in vivo and clinical studies are warranted to confirm its therapeutic value.

Keywords: *Piliostigma thonningii*, Diabetes, Inflammation, PPAR-γ, COX-2, Molecular docking.

Tropical Journal of Drug Research is indexed by Chemical Abstracts, Embase, Index Copernicus, EBSCO, African Index Medicus, JournalSeek, Directory of Open Access Journals (DOAJ), African Journal Online, Bioline International, Open-J-Gate and Pharmacy Abstracts

INTRODUCTION

Diabetes mellitus (DM) remains a significant global health burden, affecting over 537 million people worldwide, with projections indicating a rise to 783 million by 2045.[1-2] This metabolic disorder is characterized by chronic hyperglycemia, resulting from insulin resistance, impaired insulin secretion, or both, leading to severe complications such as neuropathy, nephropathy, and cardiovascular diseases.[3-4] Conventional antidiabetic therapies, including insulin and oral hypoglycemic agents, often present limitations such as adverse side effects, high costs, and reduced patient compliance.[5-6] Consequently, there is an urgent need to explore bioactive compounds from medicinal plants as alternative or complementary therapeutic options with enhanced efficacy and fewer side effects.

Piliostigma thonningii (Schumach.), a member of the Fabaceae family, is a widely distributed tropical plant renowned for its diverse ethnomedicinal applications, including the treatment of diabetes, inflammation, wounds, and microbial infections.[7-8] Several studies have identified secondary metabolites such as flavonoids, alkaloids, tannins, and saponins in *P. thonningii*, which contribute to its pharmacological properties.[9-10] However, despite its extensive traditional use, there is limited scientific validation of its antidiabetic and anti-inflammatory potential, particularly at the molecular level.

Chronic inflammation plays a pivotal role in the pathogenesis of diabetes and its complications, with pro-inflammatory cytokines such as interleukin-6 (IL-6) and tumor necrosis factor-alpha (TNF-α) exacerbating insulin resistance and pancreatic β-cell dysfunction.[11-12] Thus, the dual modulation of hyperglycemia and inflammation represents a promising therapeutic strategy for diabetes management. In vitro studies provide a reliable platform for evaluating the inhibitory effects of plant extracts on key enzymes involved in glucose metabolism, such as α-amylase and α-glucosidase, while molecular docking techniques enable the identification of specific bioactive compounds with strong binding affinities for diabetes-related protein targets.[13-14]

This study investigates the antidiabetic and anti-inflammatory potential of the ethanol extract of *Piliostigma thonningii* leaf through in vitro enzymatic assays and molecular docking analyses. By integrating experimental and computational approaches, this research aims to elucidate the underlying mechanisms of action, providing a scientific basis for the traditional use of *P. thonningii* in diabetes management and fostering the development of novel plant-based therapeutic agents.

MATERIALS AND METHODS

Chemical and Reagents

The following high-grade reagents were used in this study: 1,1-diphenyl-2-picrylhydrazyl (DPPH) alcoholic solution (≥ 98 % purity), butylated hydroxytoluene (BHT), a synthetic antioxidant (≥99%, Sigma-Aldrich, USA), ferrous sulfate heptahydrate ($FeSO_4 \cdot 7H_2O$) (≥ 98 %, Merck, Germany), hydrogen peroxide (H_2O_2) (30 % w/v, analytical grade, BDH Chemicals, UK), salicylic acid (≥ 99 %, Sigma-Aldrich, USA), sodium nitroprusside (≥ 98 %, Sigma-Aldrich, USA), Griess reagent (1 % sulfanilamide, 0.1 % naphthyl ethylenediamine dichloride in 2.5 % phosphoric acid, prepared fresh, Sigma-Aldrich, USA), glacial acetic acid (≥ 99.7 %, Fischer Scientific, UK), naphthyl ethylenediamine dichloride (≥ 98 %, Merck, Germany), phosphate buffer (0.1 M, pH 7.4, prepared using KH_2PO_4 and Na_2HPO_4, Sigma-Aldrich, USA), ascorbic acid, a synthetic antioxidant (≥ 99 %, L-ascorbic acid, Sigma-Aldrich, USA), acetate buffer (0.1 M, pH 4.5, prepared using acetic acid and sodium acetate, Sigma-Aldrich, USA), sodium acetate trihydrate (≥ 99 %, BDH Chemicals, UK), TPTZ (2,4,6-tripyridyl-s-triazine) (≥98%, Sigma-Aldrich, USA), ferric chloride hexahydrate ($FeCl_3 \cdot 6H_2O$) (≥ 97 %, Merck, Germany), potassium persulfate ($K_2S_2O_8$) (≥ 98 %, Sigma-Aldrich, USA), soluble starch (AR grade, Himedia, India), p-nitrophenyl-α-D-glucopyranoside (pNPG) (≥ 98 %, Sigma-Aldrich, USA), sodium carbonate (Na_2CO_3) (≥ 99 %, Fischer Scientific, UK), diclofenac sodium (analytical grade, ≥ 98 %, Sigma-Aldrich, USA), hypo saline (0.9 % NaCl, sterile, Thermo Fisher Scientific, USA), dimethyl sulfoxide (DMSO) (≥ 99.5 %, molecular biology grade, Sigma-Aldrich, USA), and glucose solution (5 % w/v, sterile, prepared fresh from D-glucose, Sigma-Aldrich, USA). All reagents were of analytical or molecular biology grade and used without further purification.

Collection and Identification of *Piliostigma thonningii* Leaf

The *Piliostigma thonningii* leaves was collected from Wara-Egbejila Area, Ilorin, Kwara State, Nigeria on November 29th, 2024, washed to remove dirt, and authenticated at the Department of Plant Biology, University of Ilorin, Kwara State, and a voucher number (UILH/001/926/2025) was obtained. The leaves were dried in the shade at a

low temperature to prevent degradation of bioactive compounds. The dried leaves were ground in a blender into a powder before extraction. After grinding, the powder was macerated in ethanol at room temperature for 24-48 h with constant shaking. The filtrate was concentrated on a rotatory evaporator at 40-50 °C. The resultant extract was obtained and stored in a refrigerator at 4 °C for further analysis.

***In Vitro* Studies Antidiabetics Assay**

α-Amylase inhibitory activity: α-Amylase inhibitory activity of extract and fractions was carried out according to the standard method with minor modification.[15] In a 96-well plate, reaction mixture containing 50 µl phosphate buffer (100 mM, pH = 6.8), 10 µl α–amylase (2 U/ml), and 20 µl of varying concentrations of extract and fractions (0.1, 0.2, 0.3, 0.4, and 0.5 mg/ml) was preincubated at 37 °C for 20 min. Then, the 20 µl of 1 % soluble starch (100 mM phosphate buffer pH 6.8) was added as a substrate and incubated further at 37 °C for 30 min; 100 µl of the DNS color reagent was then added and boiled for 10 min. The absorbance of the resulting mixture was measured at 540 nm using Microplate Spectrophotometer (SpectraMax 190, Molecular Devices, Sunnyvale, CA, USA). Acarbose at various concentrations (0.1–0.5 mg/ml) was used as a standard. Without test (extract and fractions) substance was set up in parallel as control and each experiment was performed in triplicates. The results were expressed as percentage inhibition, which was calculated using Equation 1.

$$\text{Inhibitory activity } (\%) = \frac{1 - \text{As}}{\text{Ac}} \times 100 \ldots\ldots\ldots Equation\ 1$$

where As is the absorbance in the presence of test substance and Ac is the absorbance of control.

α-Glucosidase inhibitory activity: α-glucosidase inhibitory activity of extract and fractions was carried out according to the standard method with minor modification.[15] In a 96-well plate, reaction mixture containing 50 µl phosphate buffer (100 mM, pH = 6. 8), 10 µl α–glucosidase (1 U/ml), and 20 µl of varying concentrations of extract and fractions (0.1, 0.2, 0.3, 0.4, and 0.5 mg/ml) was preincubated at 37 °C for 15 min. Then, 20 µl P-NPG (5 mM) was added as a substrate and incubated further at 37°C for 20 min. The reaction was stopped by adding 50 µl Na_2CO_3 (0.1 M). The absorbance of the released p-nitrophenol was measured at 405 nm using Multiskan GO Microplate Reader (Thermo Fisher Scientific, Waltham, MA, USA). Acarbose at various concentrations (0.1–0.5 mg/ml) was included as a standard. Without test substance was set up in parallel as a control and each experiment was performed in triplicates. The results were expressed as percentage inhibition, which was calculated using equation 1.

Glucose uptake capacity: This assay was performed according to the well-defined method.[16] A 1% suspension of commercial baker's yeast was prepared and allowed to rest overnight at room temperature (25 °C). The suspension was washed repeatedly and diluted to 10% (v/v). Extracts (7.125–1000 µg/mL) were dissolved in dimethyl sulfoxide, then mixed with glucose solutions of varying concentrations (5, 10, and 25 mM). After incubation at 37 °C for 10 minutes, 100 µL of yeast suspension was added, vortexed, and further incubated for 60 minutes. Absorbance was measured at 520 nm using a UV-1800 Spectrophotometer (Shimadzu, Kyoto, Japan). Metformin was used as the standard. Absorbance for the respective control was also recorded on the same wavelength. The percent increase in uptake was calculated by equation 2.

$$\text{Inhibitory activity } (\%) = \frac{A_C - A_S}{A_C} \times 100 \ldots\ldots\ldots Equation\ 2$$

where Ac is the absorbance of the control and As is the absorbance of the sample. Control is the solution having all reagents except the test sample. Metformin was used as a standard drug.

Glucose adsorption assay: The glucose adsorption capacity of the extract was determined by the method.[17] One gram of the extract was added to 100 mL of glucose solutions at different concentrations (5–30 mM) and incubated at 37 °C for 6 hours in a shaker water bath. Post-incubation, samples were centrifuged at 4800 rpm for 20 minutes. Glucose content in the supernatant was quantified using a glucose oxidase-peroxidase diagnostic kit (Randox Laboratories Ltd., UK). The amount of bound glucose was determined by the given equation 3). Here, 1 represents the glucose concentration of the original solution, while 6 represents the glucose concentration after 6 h.

$$Glucose\ Bound = \frac{G1 - G6}{Weight\ of\ sample} \times Volume\ of\ Sample \ldots\ldots\ldots Equation\ 3$$

Here, G1 represents the glucose concentration of the original solution, while G6 represents the glucose concentration after 6 h.

***In vitro* Anti-inflammatory Assay**

Protein Denaturation Assay: The inhibition of protein denaturation can be assessed using a previously modified methods.[18-19] A 1% bovine serum albumin (BSA) solution in phosphate-buffered saline (PBS, pH 6.4) was mixed with various concentrations of the extract. After incubation at 37 °C for 20 minutes, the solution was heated to 57 °C for 30 minutes. Absorbance was measured at 660 nm using the SpectraMax 190 Microplate Spectrophotometer (Molecular Devices, USA). The percentage inhibition of protein denaturation is calculated using equation 4.

$$\text{Percentage inhibition} = \frac{(\text{Absorbance of control} - \text{Absorbance of sample})}{\text{Absorbance of control}} \times 100 \ldots Equation\ 4$$

Membrane Stabilization Assay: The membrane stabilization assay is based on the prevention of hypotonicity-induced hemolysis of red blood cells (RBCs) as previously described.[20-21] Blood was collected from a healthy volunteer and washed three times with isotonic PBS. The RBC suspension is then mixed with various concentrations of the ethanol extract of *Vernonia amygdalina* and hypotonic saline. The mixture is incubated at room temperature for 10 min, followed by centrifugation at 3000 rpm for 10 min. The absorbance of the supernatant is measured at 560 nm. The percentage inhibition of hemolysis is calculated using equation 4.

Heat-Induced Hemolysis Assay: The heat-induced hemolysis assay involves incubating the RBC suspension with different concentrations of the ethanol extract of *Vernonia amygdalina* and PBS as previously described.[22] The mixtures were incubated at 54 °C for 30 min. After incubation, the samples are cooled under running tap water, centrifuged at 2500 rpm for 5 min, and the absorbance of the supernatant is measured at 560 nm. The percentage inhibition of hemolysis is calculated using equation 4.

Proteinase Inhibition Assay: The proteinase inhibition assay is performed according to the method previously described.[21] A reaction mixture of trypsin (0.06 mg), Tris-HCl buffer (20 mM, pH 7.4), and various extract concentrations was incubated at 37 °C for 5 minutes, followed by addition of 0.8% casein. After 20 minutes, the reaction was stopped using 70% trichloroacetic acid. Absorbance was measured at 210 nm using the UV-1800 Spectrophotometer (Shimadzu, Japan). The percentage inhibition of proteinase activity is calculated using equation 4.

GC-MS Analysis

GC-MS analysis of the ethanol extract was performed using an Agilent 7890A Gas Chromatograph coupled with an Agilent 7000 Triple Quadrupole Mass Spectrometer (Agilent Technologies, USA). Compounds were separated using an HP-5MS capillary column (30 m × 0.25 mm, 0.25 µm film thickness). The carrier gas was helium at a flow rate of 1 mL/min. The temperature program ramped from 100 °C to 260 °C at 4 °C/min. Injector and detector temperatures were set to 250 °C and 230 °C, respectively. Compounds were identified by comparing mass spectra with the NIST 2017 mass spectral library.[23]

In Silico Molecular Docking

In silico analysis was performed using Schrödinger Maestro v12.8 (Schrödinger, LLC, New York, NY, USA; released 2020).[24-25] Ligands were prepared using the LigPrep module with OPLS4 force field. Protein targets—PPAR-γ (PDB ID: 6ENQ) and COX-2 (PDB ID: 5F1A)—were prepared using the Protein Preparation Wizard, with protonation states optimized at pH 7.0 ± 0.2 using Epik. [26-29]

Receptor grids were generated at the active site using the Receptor Grid Generation module. High-Throughput Virtual Screening (HTVS) and Standard Precision (SP) docking were performed using Glide, and top ligands were refined with Extra Precision (XP) docking. Binding free energies (ΔG_bind) were estimated using Prime MM-GBSA.[30-34]

Visualization of binding pockets and 2D interactions was performed using BIOVIA Discovery Studio Visualizer v21.1.0.20298 (Dassault Systèmes, USA; released 2020).

Ethical Clearance

This study was conducted in accordance with the ethical principles outlined in the Declaration of Helsinki. Ethical approval for the research was obtained from the Centre for Research and Development of Kwara State University, Malete, under approval number KWASU/CR&D/REA/2024/0094, dated 6th February 2025. No human or animal subjects were harmed during this research. All procedures involving plant materials complied with institutional, national, and international guidelines.

Statistical Analysis

Statistical analysis was conducted using SPSS software (version 25.0). Data were expressed as mean ± standard deviation and analyzed using one-way analysis of variance (ANOVA) followed by Duncan's post-hoc test for multiple comparisons. A p-value < 0.05 was considered statistically

significant. IC_{50} values were calculated using GraphPad Prism 8 version 10.0.2 (Graph pad software, Inc., La Jolla, CA, USA.) statistical software.

RESULT AND DISCUSSION

In vitro Antidiabetics and Anti-inflammatory Study

The study evaluates the antidiabetic and anti-inflammatory properties of the ethanol extract of *Piliostigma thonningii* leaf through in vitro assays. The antidiabetic potential was assessed by measuring the inhibition of *α-amylase* and *α-glucosidase* activities, glucose uptake, and glucose adsorption. The anti-inflammatory properties were determined by analyzing the inhibition of protein denaturation, proteinase activity, membrane stabilization, and heat-induced hemolysis.

For the antidiabetic assays, the extract exhibited a dose-dependent inhibition of *α-amylase* and *α-glucosidase* activities, with IC_{50} values of 68.50±1.84 µg/ml and 483.70±2.69 µg/ml, respectively (Figure 1). The extract showed a lower inhibitory effect on *α-amylase* compared to acarbose (IC_{50} = 16.63±1.22 µg/ml) but was more effective against *α-glucosidase* than acarbose (IC_{50} = 512.30±2.71 µg/ml). Additionally, the extract enhanced glucose uptake (IC_{50} = 78.78±1.89 µg/ml) and glucose adsorption (IC_{50} = 43.83±1.89 µg/ml), though less effective than metronidazole (IC_{50} = 20.96±1.32 µg/ml).

Regarding anti-inflammatory activities, the extract demonstrated notable inhibition of protein denaturation (IC_{50} = 61.50±1.79 µg/ml), proteinase activity (IC_{50} = 63.30±1.80 µg/ml), membrane stabilization (IC_{50} = 58.37±1.77 µg/ml), and heat-induced hemolysis (IC_{50} = 83.97±1.92 µg/ml) (Figure 2). These effects were less potent than diclofenac, which had lower IC_{50} values across all parameters. However, the results suggest that the extract still possesses significant anti-inflammatory potential.

The results aligned with earlier reports linking polyphenol-rich medicinal plants to glycemic regulation.[35-36] While the extract exhibited weaker α-amylase inhibition than the standard drug acarbose, it showed greater potency against α-glucosidase. This selectivity is beneficial, as strong α-amylase inhibition is associated with gastrointestinal side effects. These findings suggest that *P. thonningii* may offer a safer, more targeted approach to postprandial glucose control.[37-39] These findings suggest that *P. thonningii* may offer a safer, more targeted approach to postprandial glucose control.

GC-MS Result of Ethanol Extract of *Piliostigma thonningii* Leaf

The GC-MS chromatogram of P. thonningii leaf extract, revealing a complex profile of 79 phytochemicals. Notably, compounds such as anthracene, 1,2,3,4-tetrahydro-9,10-dimethyl, butylated hydroxytoluene, phthalic acid derivatives, and long-chain alkanes and esters were identified, many of which possess documented antidiabetic and anti-inflammatory properties (Figure 3, Table 1).

Key compounds of interest include alkanes (e.g., Heptacosane, $C_{27}H_{56}$), esters (e.g., Dibutyl phthalate, $C_{16}H_{22}O_4$), fatty acid derivatives (e.g., Oleic Acid, $C_{18}H_{34}O_2$), and fluorinated organics (e.g., Dotriacontyl heptafluorobutyrate, $C_{36}H_{59}F_7O_2$). Notably, antioxidants such as Butylated Hydroxytoluene ($C_{15}H_{24}O$) and pharmaceutically relevant phthalates (e.g., Bis(2-ethylhexyl) phthalate, $C_{24}H_{38}O_4$) were identified, highlighting the plant's potential bioactive properties. Structural diversity is evident across aliphatic hydrocarbons, branched alkanes, and complex esters, reflecting the phytochemical richness of *P. thonningii*.

The molecular weights range from 130.23 g/mol (2-ethyl-1-hexanol) to 942.30 g/mol (1-chlorohexatriacontyl pentafluoropropionate), demonstrating significant variability in compound sizes and functional groups. For precise validation, researchers are advised to consult PubChem entries using the provided CID numbers. This dataset serves as a critical reference for phytochemical, pharmacological, and environmental studies focused on *P. thonningii* or related species.

Molecular Docking Study

The molecular docking study of the ethanol extract of *Piliostigma thonningii* leaf was conducted to assess its antidiabetic and anti-inflammatory potential through interactions with peroxisome proliferator-activated receptor gamma (PPAR-γ) and human cyclooxygenase-2 (COX-2). PPAR-γ plays a critical role in glucose and lipid metabolism, making it a target for antidiabetic therapies, while COX-2 is an enzyme responsible for prostaglandin synthesis and is a key target in anti-inflammatory drug development. The High-Throughput Virtual Screening (HTVS) results, summarized in Table 2 and Table 3, demonstrate that several phytochemicals from *P. thonningii* exhibit strong binding affinities with these targets, with comparable or superior Glide GScores to standard reference drugs such as pioglitazone (antidiabetic) and celecoxib (anti-inflammatory).

Notably, anthracene, 1,2,3,4-tetrahydro-9,10-dimethyl- exhibited the best interaction with PPAR-γ (-7.24 kcal/mol), while tetratriacontyl trifluoroacetate displayed a significant binding affinity with COX-2 (-6.40 kcal/mol), supporting the pharmacological potential of these compounds.

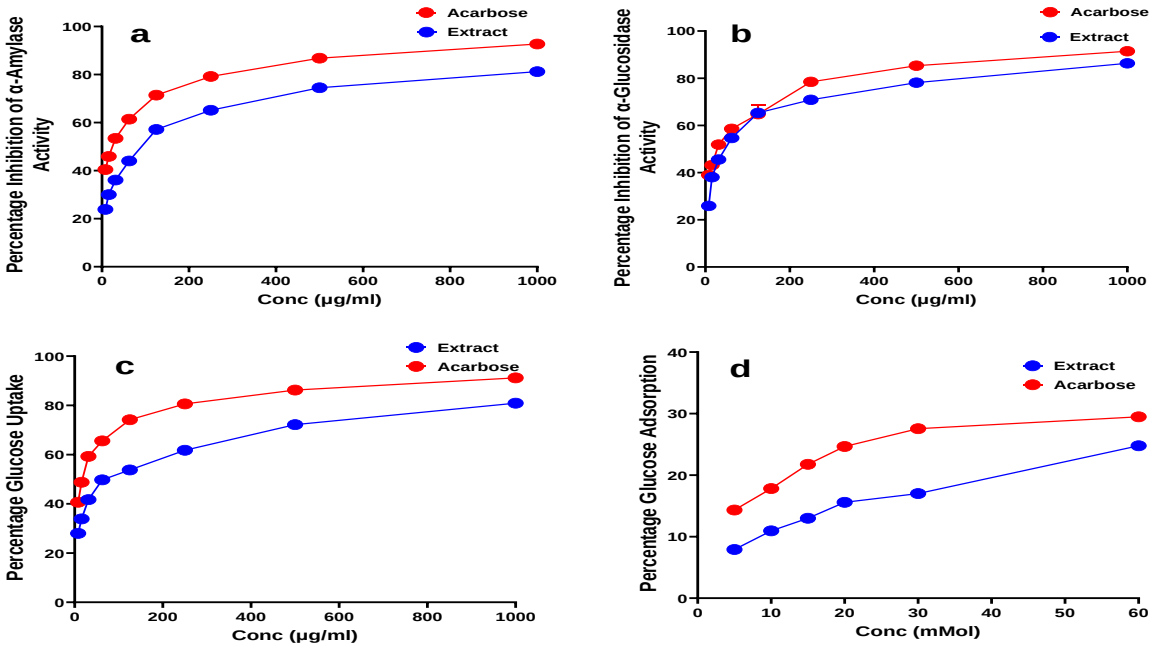

Figure 1: Percentage inhibition of (a) α-amylase and (b) α-glucosidase and (c) percentage glucose uptake and (d) percentage glucose adsorption of the extract.
IC_{50} α-Amylase: Extract – 68.50±1.84 µg/ml, Acarbose – 16.63±1.22 µg/ml, α-Glucosidase: Extract – 483.70±2.69 µg/ml, Acarbose – 512.30±2.71 µg/ml, G. uptake: Extract – 78.78±1.89 µg/ml, Metronidazole – 20.96±1.32 µg/ml,G. adsorption: Extract – 43.83±1.89 µg/ml, Metronidazole – 20.96±1.32 µg/ml

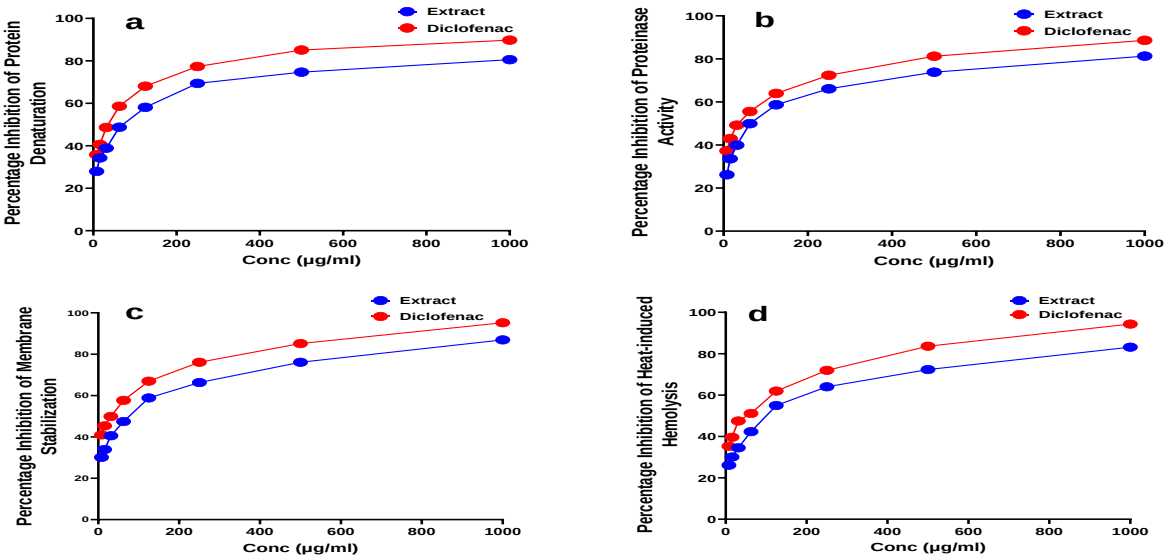

Figure 2: Percentage inhibition of (a) protein denaturation (b) proteinase (c) membrane stabilization and (d) heat-induced hemolysis by the extract. IC_{50} PD: Extract – 61.50±1.79 µg/ml, Diclofenac – 29.45±1.47 µg/ml, PI: Extract – 63.30±1.80 µg/ml, Diclofenac – 30.33±1.48 µg/ml, MS: Extract – 58.37±1.77 µg/ml, Diclofenac – 24.37±1.39 µg/ml, HIH: Extract – 83.97±1.92 µg/ml, Diclofenac – 36.26±1.51 µg/ml

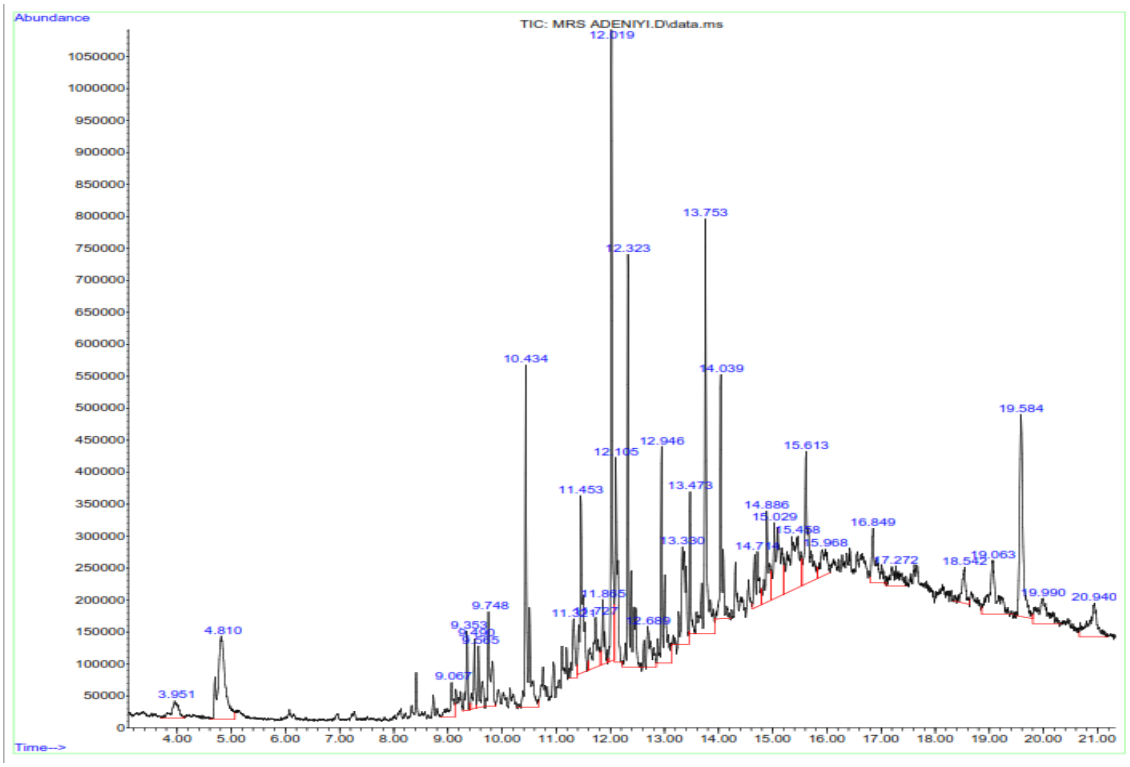

Figure 3: GC-MS Chromatogram of *Piliostigma thonningii* leaf

Table 1: GC-MS Analysis Results of *Piliostigma thonningii* leaf

Peak No	S No	Ligand	Retention time	Area	Quality	Molecular Formula	Molecular Weight (g/mol)	CID
1	1	1-Hexanol, 2-ethyl-	3.951	0.96	35	$C_8H_{18}O$	130.23	7720
1	2	2-Dodecanol	3.951	0.96	32	$C_{12}H_{26}O$	186.34	25045
2	3	Benzoic acid, methyl ester	4.810	4.95	49	$C_8H_8O_2$	136.15	7150
3	4	Heptadecane, 2,6,10,15-tetramethyl	9.067	1.05	89	$C_{21}H_{44}$	296.58	41209
3	5	Decane, 2-methyl-	9.067	1.05	58	$C_{11}H_{24}$	156.31	23415
4	6	Octadecane, 3-ethyl-5-(2-ethylbutyl)	9.353	1.07	86	$C_{26}H_{54}$	362.72	292285
4	7	Heptacosane	9.353	1.07	72	$C_{27}H_{56}$	380.74	11636
4	8	Hexacosane	9.353	1.07	72	$C_{26}H_{54}$	366.72	12407
5	9	10-Methylnonadecane	9.490	0.96	86	$C_{20}H_{42}$	282.50	530070
5	10	Hexadecane	9.490	0.96	80	$C_{16}H_{34}$	226.44	11006
5	11	Tetradecane	9.490	0.96	72	$C_{14}H_{30}$	198.39	12389
6	12	Butylated Hydroxytoluene	9.565	1.10	97	$C_{15}H_{24}O$	220.35	31404
7	13	Dodecanoic acid, methyl ester	9.748	2.04	94	$C_{13}H_{26}O_2$	214.34	8139
8	14	9-Eicosene, (E)-	10.434	5.58	94	$C_{20}H_{38}$	278.52	5365037
8	15	3-Eicosene, (E)-	10.434	5.58	91	$C_{20}H_{38}$	278.52	5365051
8	16	7-Heptadecene, 1-chloro-	10.434	5.58	91	$C_{17}H_{31}Cl$	274.89	5364485
9	17	2-(2-Bromoethyl)-3-methyl-oxirane	11.321	1.28	30	$C_6H_{11}BrO$	165.03	558912
9	18	6-Tetradecanesulfonic acid, butyl ester	11.321	1.28	30	$C_{18}H_{38}O_3S$	334.56	551402
9	19	(4-Acetylphenyl) phenylmethane	11.321	1.28	25	$C_{15}H_{14}O$	210.27	258457
10	20	10-Methylnonadecane	11.453	4.05	90	$C_{20}H_{42}$	282.50	530070
10	21	Octacosane	11.453	4.05	90	$C_{28}H_{58}$	394.80	12408

10	22	2-methyloctacosane	11.453	4.05	90	$C_{29}H_{60}$	408.80	519147
11	23	Oxalic acid, allyl octadecyl ester	11.727	1.84	38	$C_{23}H_{42}O_4$	382.60	6420237
11	24	Benzene, (1-pentylheptyl)-	11.727	1.84	38	$C_{18}H_{30}$	246.40	17629
11	25	Dodecane	11.727	1.84	22	$C_{12}H_{26}$	170.33	8182
12	26	6-Tetradecanesulfonic acid,butyl ester	11.865	1.12	87	$C_{18}H_{38}O_3S$	334.60	551402
12	27	2-Methyltetracosane	11.865	1.12	87	$C_{25}H_{52}$	352.70	527459
12	28	Tetratetracontane	11.865	1.12	83	$C_{44}H_{90}$	619.20	23494
13	29	1,1'-Biphenyl, 2,2',5,5'-tetramethyl-	12.019	7.56	90	$C_{16}H_{18}$	210.31	137818
13	30	Anthracene, 1,2,3,4-tetrahydro-9,10-dimethyl-	12.019	7.56	78	$C_{16}H_{18}$	210.31	610936
14	31	1,1'-Biphenyl, 3,3',4,4'-tetramethyl-	12.105	3.46	70	$C_{16}H_{18}$	210.31	21029
14	32	1,1'-Biphenyl, 3,4-diethyl-	12.105	3.46	60	$C_{16}H_{18}$	210.31	43551
15	33	1-Nonadecene	12.323	6.50	94	$C_{19}H_{38}$	266.50	29075
15	34	E-14-Hexadecenal	12.323	6.50	91	$C_{16}H_{30}O$	238.41	5363106
16	35	Carbonic acid, octadecyl vinyl ester	12.689	1.66	62	$C_{20}H_{38}O_3$	338.53	91693138
16	36	Carbonic acid, octadecyl prop-1-en-2-yl ester	12.689	1.66	58	$C_{22}H_{42}O_3$	354.60	91692938
16	37	Carbonic acid, hexadecyl prop-1-en-2-yl ester	12.689	1.66	53	$C_{20}H_{38}O_3$	326.50	91692933
17	38	Phthalic acid, hexadecyl propyl ester	12.946	4.43	80	$C_{27}H_{44}O_4$	432.60	6423375
17	39	Phthalic acid, propyl nonyl ester	12.946	4.43	80	$C_{20}H_{30}O_4$	334.40	525243
17	40	Phthalic acid, ethyl octadecyl ester	12.946	4.43	82	$C_{28}H_{46}O_4$	446.70	6423932
18	41	Heneicosane	13.330	3.58	80	$C_{21}H_{44}$	296.60	12403
18	42	5-Ethyl-5-methylnonadecane	13.330	3.58	80	$C_{22}H_{46}$	310.60	53839399
18	43	Heptadecane	13.330	3.58	72	$C_{17}H_{36}$	240.50	12398
19	44	Hexadecanoic acid, methyl ester	13.473	1.48	95	$C_{17}H_{34}O_2$	270.45	8181
19	45	Pentadecanoic acid, 14-methyl-, methyl ester	13.473	1.48	94	$C_{17}H_{34}O_2$	270.50	21205
20	46	Dibutyl phthalate	13.753	6.94	90	$C_{16}H_{22}O_4$	278.34	3026
20	47	Di-sec-butyl phthalate	13.753	6.94	86	$C_{16}H_{22}O_4$	278.34	249496
20	48	Phthalic acid, butyl hexyl ester	13.753	6.94	78	$C_{18}H_{26}O_4$	306.40	526381
21	49	2- Chloropropionic acid, octadecyl ester	14.039	3.42	91	$C_{21}H_{41}ClO_2$	361.00	522892
21	50	1-Nonadecene	14.039	3.42	91	$C_{19}H_{38}$	266.50	29075
21	51	Heptadecyl heptafluorobutyrate	14.039	3.42	90	$C_{21}H_{35}F_7O_2$	452.50	545577
22	52	Dotriacontyl heptafluorobutyrate	14.714	1.77	46	$C_{36}H_{65}F_7O_2$	662.90	91692956
22	53	Tetratriacontyl pentafluoropropionate	14.714	1.77	46	$C_{37}H_{69}F_5O_2$	640.90	91693161
23	54	1,19-Eicosadiene	14.886	2.20	86	$C_{20}H_{38}$	278.51	519006
23	55	Oleic Acid	14.886	2.20	86	$C_{18}H_{34}O_2$	282.50	445639
23	56	1-Dodecanol, 2-hexyl-	14.886	2.20	76	$C_{18}H_{38}O$	270.50	86112
24	57	Carbonic acid, eicosyl vinyl ester	15.029	3.76	90	$C_{23}H_{42}O_3$	366.60	91693137
24	58	Eicosyl isobutyl ether	15.029	3.76	87	$C_{24}H_{50}O$	354.70	91693109
24	59	Nonahexacontanoic acid	15.029	3.76	86	$C_{69}H_{138}O_2$	999.80	38626
25	60	Octadecane, 1-chloro-	15.458	4.75	86	$C_{18}H_{37}Cl$	288.95	18815
25	61	Hexatriacontyl pentafluoropropionate	15.458	4.75	76	$C_{39}H_{73}F_5O_2$	686.91	91693081
26	62	1-Heptacosanol	15.613	3.74	87	$C_{27}H_{56}O$	396.70	74822
26	63	1-Hexacosanol	15.613	3.74	83	$C_{26}H_{54}O$	382.70	68171
26	64	Nonacos-1-ene	15.613	3.74	81	$C_{29}H_{58}$	406.70	156989
27	65	Octadecane, 1-chloro-	15.968	1.36	92	$C_{18}H_{37}Cl$	288.90	18815
27	66	Tetratriacontyl trifluoroacetate	15.968	1.36	78	$C_{36}H_{69}F_3O_2$	604.87	91692947

28	67	Tetratriacontyl heptafluorobutyrate	16.849	1.83	83	$C_{38}H_{69}F_7O_2$	690.90	91692919
28	68	Tetratriacontyl pentafluoropropionate	16.849	1.83	83	$C_{37}H_{63}F_5O_2$	640.90	91693161
29	69	Octatriacontyl pentafluoropropionate	17.272	1.29	83	$C_{41}H_{77}F_5O_2$	697.00	91693082
30	70	1,3-Dioxolane, 4-ethyl-5-octyl-2,2-bis(trifluoromethyl)-, cis-	18.542	1.12	46	$C_{15}H_{24}F_6O_2$	350.34	91694991
30	71	Cyclopentane, 1,1'-[3-(2-cyclopentylethyl)-1,5-pentanediyl]bis-	18.542	1.12	46	$C_{25}H_{40}$	304.60	281840
30	72	2-Propanone, 1,1,1,3,3,3-hexafluoro-	18.542	1.12	43	C_3F_6O	166.02	12695
31	73	Hexatriacontyl pentafluoropropionate	19.063	3.31	55	$C_{39}H_{73}F_5O_2$	669.00	91693081
32	74	Diisooctyl phthalate	19.584	5.53	83	$C_{24}H_{38}O_4$	390.60	33934
32	75	Bis(2-ethylhexyl) phthalate	19.584	5.53	80	$C_{24}H_{38}O_4$	390.60	8343
32	76	Phthalic acid, 2-ethylhexyl isohexyl ester	19.584	5.53	72	$C_{22}H_{34}O_4$	362.50	8343
33	77	Octatriacontyl trifluoroacetate	19.990	2.10	62	$C_{40}H_{77}F_3O_2$	647.00	91693163
33	78	Triacontyl trifluoroacetate	19.990	2.10	35	$C_{32}H_{61}F_3O_2$	534.80	91693300
33	79	Triacontyl pentafluoropropionate	19.990	2.10	35	$C_{33}H_{61}F_5O_2$	584.80	91692951

Further computational analysis was conducted using Standard Precision (SP) and Extra Precision (XP) molecular docking simulations, as shown in Table 4 and Table 5. These results provide a deeper understanding of the ligand-receptor interactions by integrating MM-GBSA (Molecular Mechanics/Generalized Born Surface Area) energy calculations. Among the compounds tested against PPAR-γ, phthalic acid, propyl nonyl ester, and cyclopentane, 1,1'-[3-(2-cyclopentylethyl)-1,5-pentanediyl]bis- demonstrated the highest binding affinities, with MM-GBSA values of -62.00 and -47.65 kcal/mol, respectively. Interestingly, the reference drug pioglitazone had a slightly weaker MM-GBSA score (-59.53 kcal/mol), indicating that *P. thonningii* phytochemicals might serve as promising alternatives in diabetes management. Similarly, for COX-2 inhibition, octatriacontyl trifluoroacetate and hexatriacontyl pentafluoropropionate exhibited strong affinities (-48.79 and -57.83 kcal/mol, respectively), reinforcing their potential as anti-inflammatory agents.

Figure 4 provides 2D interaction diagrams showing the molecular docking between PPAR-γ and lead phytochemicals from *P. thonningii*. Sub-figure 4a shows phthalic acid, propyl nonyl ester forming stable hydrogen bonds and hydrophobic interactions within the PPAR-γ binding pocket, with favorable XP docking and MM-GBSA scores. Figure 4b illustrates cyclopentane, 1,1'-[3-(2-cyclopentylethyl)-1,5-pentanediyl]bis-, which exhibited strong binding energy (XP GScore: –6.95 kcal/mol), suggesting its structural compatibility with the receptor. Figure 4c shows dibutyl phthalate, a known anti-inflammatory agent, interacting with polar residues, while Figure 4d (reference drug pioglitazone) helps validate these interactions by comparison.

Figure 5 visualizes the binding interactions between COX-2 and selected *P. thonningii* compounds. Sub-figure 5a depicts octatriacontyl trifluoroacetate, which displayed strong XP binding affinity (–1.43 kcal/mol) and favorable MM-GBSA energy, interacting predominantly via van der Waals forces. Figure 5b shows hexatriacontyl pentafluoropropionate, another potent candidate with XP GScore of –2.81 kcal/mol and notable interaction with the COX-2 active site. Figure 5c reveals 2-methyloctacosane's modest interaction profile, while Figure 5d (celecoxib reference) provides a benchmark for validating docking behavior.

Molecular docking results further support the antidiabetic activity of the extract. Several bioactive compounds exhibited strong binding affinities to peroxisome proliferator-activated receptor gamma (PPAR-γ), a critical target in glucose and lipid metabolism. Among them, anthracene, 1,2,3,4-tetrahydro-9,10-dimethyl- showed the highest docking score of –7.24 kcal/mol, outperforming the reference drug pioglitazone (–5.64 kcal/mol).

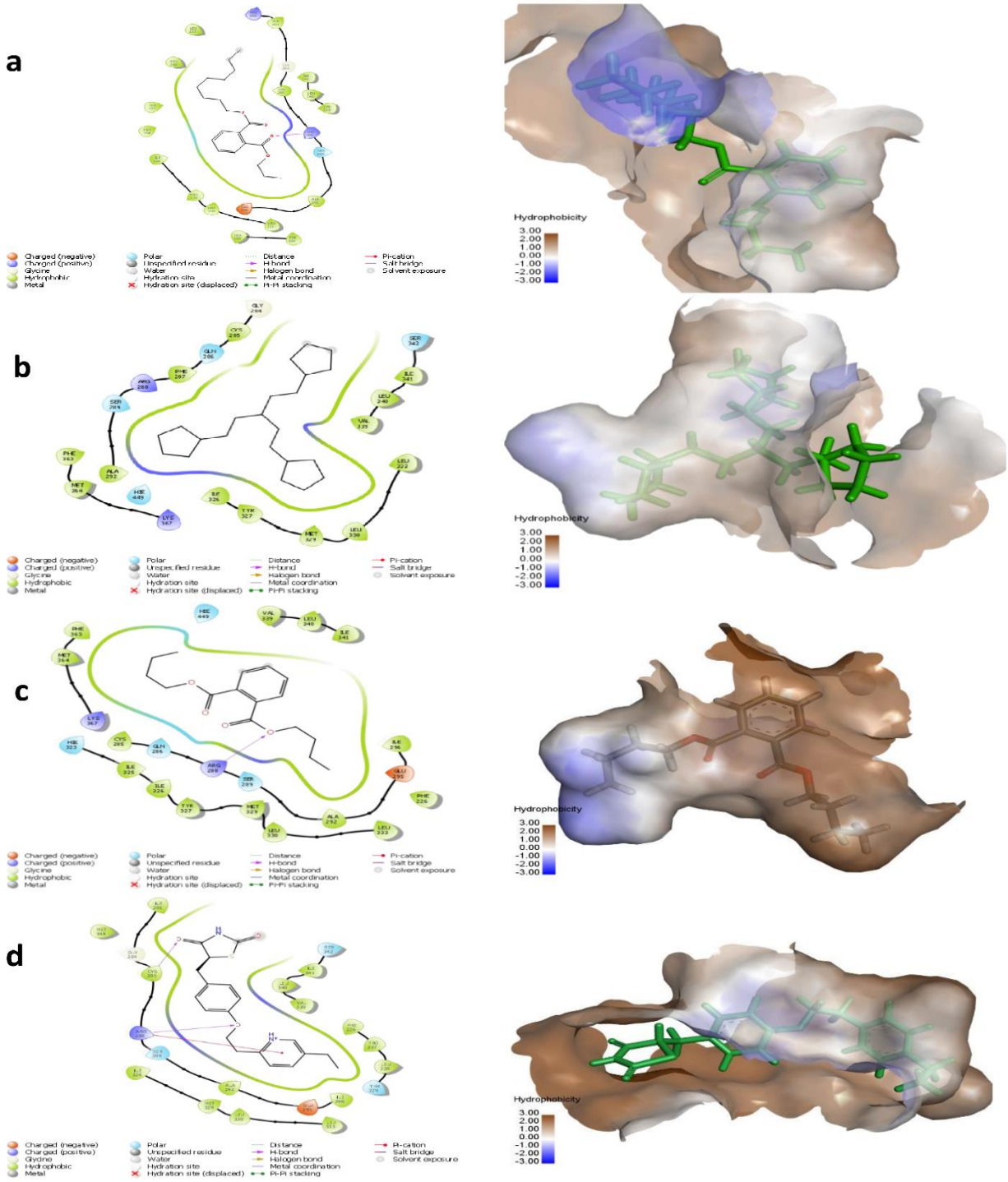

Figure 4: Binding pocket and two-dimensional interactions between PPAR-γ and *P. thonningii* compounds. This figure presents a detailed view of the binding pocket and two-dimensional interactions between PPAR-γ and three *P. thonningii* lead compounds: (a) Phthalic acid, propyl nonyl ester; (b) Cyclopentane, 1,1'-[3-(2-cyclopentylethyl)-1,5-pentanediyl]bis-; and (c) Dibutyl phthalate plus reference drug: (d) Pioglitazone. These interactions are elucidated following glide quantum polarized ligand docking, offering insights into the molecular dialogue between these phytochemicals and the active site amino acids of PPAR-γ.

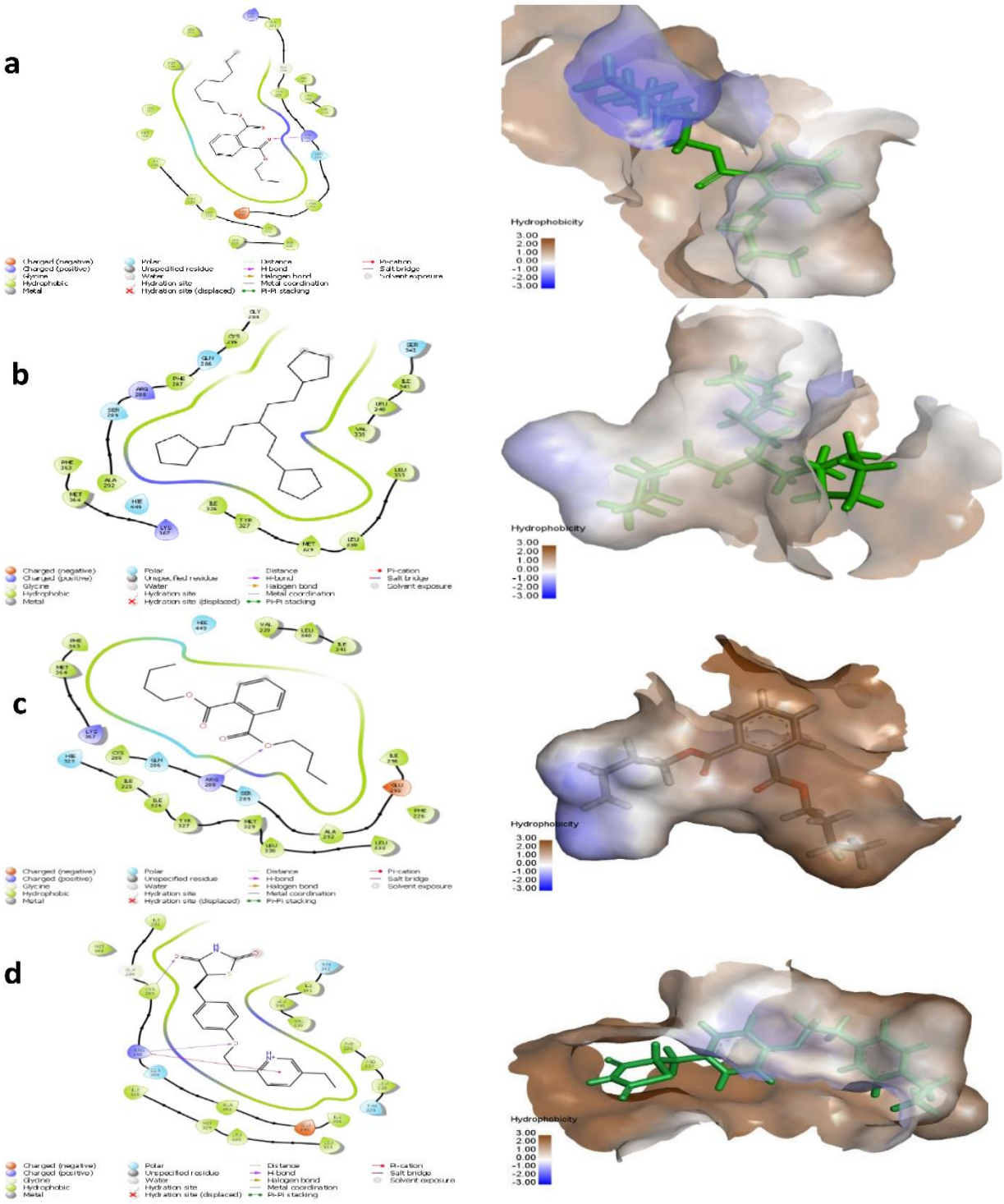

Figure 5: Binding pocket and two-dimensional interactions between COX-2 and *P. thonningii* compounds. This figure presents a detailed view of the binding pocket and two-dimensional interactions between COX-2 and three *P. thonningii* lead compounds: (a) Octatriacontyl trifluoroacetate; (b) Hexatriacontyl pentafluoropropionate; and (c) 2-methyloctacosane plus reference drug: (d) Celecoxib. These interactions are elucidated following glide quantum polarized ligand docking, offering insights into the molecular dialogue between these phytochemicals and the active site amino acids of COX-2.

The compound formed stable hydrogen bonds and hydrophobic interactions within the PPAR-γ binding site, comparable to known natural PPAR-γ agonists.[40-41] This highlights the potential of *P. thonningii* as a promising source of novel PPAR-γ modulators that may offer safer alternatives to synthetic thiazolidinediones, which are often associated with cardiovascular risks.[42-43]

In addition to its antidiabetic effects, *P. thonningii* demonstrated notable anti-inflammatory activity. The extract effectively inhibited protein denaturation ($IC_{50} = 61.50 \pm 1.79$ µg/mL) and proteinase activity ($IC_{50} = 63.30 \pm 1.80$ µg/mL), reflecting its ability to suppress inflammatory protein responses. These outcomes are consistent with other studies involving medicinal plants known for their anti-inflammatory properties.[44-45]

Molecular docking analysis supported these in vitro findings, revealing strong interactions between bioactive compounds and cyclooxygenase-2 (COX-2), a key enzyme involved in the inflammatory cascade. Specifically, tetratriacontyl trifluoroacetate (–6.40 kcal/mol) and hexatriacontyl pentafluoropropionate (–5.43 kcal/mol) demonstrated binding affinities approaching that of the reference drug celecoxib (–7.13 kcal/mol). These compounds displayed stable binding within the COX-2 active site, suggesting their potential as natural COX-2 inhibitors with reduced gastrointestinal side effects.[46-47]

Collectively, these findings indicate that *P. thonningii* operates via a dual mechanism—modulating both glucose metabolism and inflammatory responses. This supports its traditional use in managing diabetes and related inflammatory conditions.[48-49] Given the well-established link between chronic inflammation and insulin resistance,[50] the dual pharmacological profile of *P. thonningii* enhances its appeal as a candidate for multifunctional phytotherapeutic development.

Furthermore, GC-MS analysis identified several bioactive constituents—including flavonoids, phenolic acids, and phthalates—known for their antidiabetic and anti-inflammatory properties.[51-52] These compounds likely contribute to the extract's observed biological activities and provide a basis for future drug discovery and development.

CONCLUSION

In conclusion, the combined in vitro and molecular docking analyses provide robust evidence for the antidiabetic and anti-inflammatory potential of *Piliostigma thonningii*. Its selective inhibition of α-glucosidase, strong binding affinities to PPAR-γ and COX-2, and a favorable bioactive compound profile highlight its therapeutic relevance and potential as a natural treatment candidate. While these findings are encouraging, further investigations—particularly comprehensive in vivo studies and well-structured clinical trials—are essential to establish its pharmacological efficacy and safety in human models. Looking ahead, Structure-Activity Relationship (SAR) studies could be employed to optimize the lead compounds for enhanced potency, selectivity, and bioavailability. Moreover, future research may explore advanced drug formulation strategies, such as nanoencapsulation, to improve the delivery and stability of these phytochemicals. Genomic and metabolomic approaches may also uncover underlying biosynthetic pathways, enabling biotechnological production of key bioactives. Ultimately, this study lays a foundation for the development of novel plant-derived therapeutics and exemplifies the value of integrating computational and experimental methodologies in natural product drug discovery.

CONFLICT OF INTEREST

The authors declare no conflict of interest.

AUTHORS DECLARATION

The authors hereby declare that the works presented in this article are original and that any liability for claims relating to the content of this article will be borne by them.

ACKNOWLEDGMENT

The Authors thank Miss Iwinosa Success Emovon and Miss Jennifer Ogbeifun for their contributions to the experimental phase of this study

REFERENCES

1. Ong KL, Stafford LK, McLaughlin SA, Boyko EJ, Vollset SE, Smith AE. Global, regional, and national burden of diabetes from 1990 to 2021, with projections of prevalence to 2050: a systematic analysis for the Global Burden of Disease Study 2021. Lancet. 2023;402(10397):203-234. Doi: 10.1016/S0140-6736(23)01301-6
2. Hossain MJ, Al-Mamun M, Islam MR. Diabetes mellitus, the fastest growing global public health concern: Early detection should be focused. Health Sci Rep. 2024;7(3):e2004. Doi: 10.1002/hsr2.2004
3. Antar SA, Ashour NA, Sharaky M, Khattab M, Ashour NA, Zaid RT. Diabetes mellitus: Classification, mediators, and complications; A gate to identify potential targets for the development of new effective treatments. Biomed Pharmacother. 2023;168:115734. Doi: 10.1016/j.biopha.2023.115734
4. Banday MZ, Sameer AS, Nissar S. Pathophysiology of diabetes: An overview. Avicenna J Med. 2020;10(4):174-188. Doi: 10.4103/ajm.ajm_53_20
5. Chaudhury A, Duvoor C, Reddy Dendi VS, Kraleti S, Chada A, Ravilla R. Clinical Review of Antidiabetic Drugs: Implications for Type 2 Diabetes Mellitus Management. Front Endocrinol (Lausanne). 2017;8:6. Doi: 10.3389/fendo.2017.00006
6. Hermansen K, Mortensen LS, Hermansen ML. Combining insulins with oral antidiabetic agents: effect on hyperglycemic control, markers of cardiovascular risk and disease. Vasc Health Risk Manag. 2008;4(3):561-574. Doi: 10.2147/vhrm.s1815
7. Nethathe B, Ramphinwa LM, Selekane Motadi A, Matlakala FK. Scoping review of ethnobotanical studies on *Piliostigma thonningii* (Schumach.) Milne-Redh. in Sub-Saharan Africa. Front Pharmacol. 2025; 16:1575548. Doi: 10.3389/fphar.2025.1575548
8. Abubakar IB, Malami I, Muhammad A, Salihu Shinkafi T, Shehu D, Maduabuchi Aja P. A review of the medicinal uses and biological activity of *Piliostigma thonningii* (Schum). Milne-Redh. RPSPPR 2024;3(1). Doi: 10.1093/rpsppr/rqae004
9. Teoh ES. Secondary Metabolites of Plants. Medicinal Orchids of Asia. 2015:57-73.
10. Pathak G. Chapter 14 - Biological production and application of secondary metabolites and other medicinal products. In: Singh DB, Upadhyay SK, editors. Medicinal Biotechnology: Academic Press; 2025. p. 273-325. Doi: 10.1016/B978-0-443-22264-1.00014-1
11. Tsalamandris S, Antonopoulos AS, Oikonomou E, Papamikroulis GA, Vogiatzi G, Papaioannou S. The Role of Inflammation in Diabetes: Current Concepts and Future Perspectives. Eur Cardiol. 2019;14(1):50-59. Doi: 10.15420/ecr.2018.33.1
12. Nedosugova LV, Markina YV, Bochkareva LA, Kuzina IA, Petunina NA, Yudina IY. Inflammatory Mechanisms of Diabetes and Its Vascular Complications. Biomedicines. 2022;10(5). Doi: 10.3390/biomedicines10051168
13. Prpa EJ, Bajka BH, Ellis PR, Butterworth PJ, Corpe CP, Hall WL. A systematic review of in vitro studies evaluating the inhibitory effects of polyphenol-rich fruit extracts on carbohydrate digestive enzymes activity: a focus on culinary fruits consumed in Europe. Crit Rev Food Sci Nutr. 2021;61(22):3783-3803. Doi: 10.1080/10408398.2020.1808585
14. Adisakwattana S, Ruengsamran T, Kampa P, Sompong W. *In vitro* inhibitory effects of plant-based foods and their combinations on intestinal α-glucosidase and pancreatic α-amylase. BMC Complement Altern Med. 2012;12(1):110. Doi: 10.1186/1472-6882-12-110
15. Telagari M, Hullatti K. *In-vitro* α-amylase and α-glucosidase inhibitory activity of *Adiantum caudatum* Linn. and *Celosia argentea* Linn. extracts and fractions. Indian J Pharmacol. 2015;47(4):425-429. Doi: 10.4103/0253-7613.161270
16. Patil A, Dwivedi PSR, Gaonkar SN, Kumbhar V, Shankar Madiwalar V, Khanal P. GLUT-2 mediated glucose uptake analysis of *Duranta repens*: In-silico and In-vitro approach. J Diabetes Metab Disord. 2022;21(1):419-427. Doi: 10.1007/s40200-022-00988-3

17. Ahmed F, Sairam S, Urooj A. *In vitro* hypoglycemic effects of selected dietary fiber sources. J Food Sci Technol. 2011;48(3):285-289. Doi: 10.1007/s13197-010-0153-7
18. Tanford C. Protein Denaturation. In: Anfinsen CB, Anson ML, Edsall JT, Richards FM, editors. Advances in Protein Chemistry. 23: Academic Press; 1968. p. 121-282. Doi: 10.1016/S0065-3233(08)60401-5
19. Roth GA, Mensah GA, Johnson CO, Addolorato G, Ammirati E, Baddour LM. Global Burden of Cardiovascular Diseases and Risk Factors, 1990–2019: Update From the GBD 2019 Study. JACC. 2020;76(25):2982-3021. Doi: 10.1016/j.jacc.2020.11.010
20. Yesmin S, Paul A, Naz T, Rahman ABMA, Akhter SF, Wahed MII. Membrane stabilization as a mechanism of the anti-inflammatory activity of ethanolic root extract of Choi (*Piper chaba*). Clin Phytoscience. 2020;6(1):59. Doi: 10.1186/s40816-020-00207-7
21. Ameena A, Meignana AA, Karthikeyan R, Rajeshkumar S. Evaluation of the Anti-inflammatory, Antimicrobial, Antioxidant, and Cytotoxic Effects of Chitosan Thiocolchicoside-Lauric Acid Nanogel. Cureus. 2023;15(9):e46003. Doi: 10.7759/cureus.46003
22. Anosike CA, Obidoa O, Ezeanyika LU. Membrane stabilization as a mechanism of the anti-inflammatory activity of methanol extract of garden egg (*Solanum aethiopicum*). Daru. 2012;20(1):76. Doi: 10.1186/2008-2231-20-76
23. Koo I, Kim S, Zhang X. Comparative analysis of mass spectral matching-based compound identification in gas chromatography-mass spectrometry. J Chromatogr A. 2013;1298:132-138. Doi: 10.1016/j.chroma.2013.05.021
24. Gonfa YH, Tessema FB, Bachheti A, Rai N, Tadesse MG, Nasser Singab A. Anti-inflammatory activity of phytochemicals from medicinal plants and their nanoparticles: A review. Curr Res Biotechnol. 2023;6:100152. Doi: 10.1016/j.crbiot.2023.100152
25. Kumar A, P N, Kumar M, Jose A, Tomer V, Oz E. Major Phytochemicals: Recent Advances in Health Benefits and Extraction Method. Molecules. 2023;28(2). Doi: 10.3390/molecules28020887
26. Kim S. Exploring Chemical Information in PubChem. Curr Protoc. 2021;1(8):e217.
27. Kim S, Thiessen PA, Bolton EE, Chen J, Fu G, Gindulyte A. PubChem Substance and Compound databases. Nucleic Acids Res. 2016;44(D1):D1202-D1213. Doi: 10.1093/nar/gkv951
28. Lindert S, Durrant JD, McCammon JA. LigMerge: a fast algorithm to generate models of novel potential ligands from sets of known binders. Chem Biol Drug Des. 2012;80(3):358-865. Doi: 10.1111/j.1747-0285.2012.01414.x
29. Shelley JC, Cholleti A, Frye LL, Greenwood JR, Timlin MR, Uchimaya M. Epik: a software program for pKaprediction and protonation state generation for drug-like molecules. J Comput Aided Mol Des. 2007;21(12):681-691. Doi: 10.1007/s10822-007-9133-z
30. Eema M, Avupati VR. In silico binding role of flavonoids as SARS-CoV-2 main protease (Mpro) inhibitors: A dataset of molecular docking simulation-based high-throughput virtual screening (HTVS). Data in Brief. 2025;59:111308. Doi: 10.1016/j.dib.2025.111308
31. Shamsian S, Sokouti B, Dastmalchi S. Benchmarking different docking protocols for predicting the binding poses of ligands complexed with cyclooxygenase enzymes and screening chemical libraries. Bioimpacts. 2024;14(2):29955. Doi: 10.34172/bi.2023.29955
32. Rifai EA, van Dijk M, Vermeulen NPE, Yanuar A, Geerke DP. A Comparative Linear Interaction Energy and MM/PBSA Study on SIRT1-Ligand Binding Free Energy Calculation. J Chem Inf Model. 2019;59(9):4018-4033. Doi: 10.1021/acs.jcim.9b00609
33. Dong L, Qu X, Zhao Y, Wang B. Prediction of Binding Free Energy of Protein-Ligand Complexes with a Hybrid Molecular Mechanics/Generalized Born Surface Area and Machine Learning Method. ACS Omega. 2021;6(48):32938-32947. Doi: 10.1021/acsomega.1c04996
34. Genheden S, Ryde U. The MM/PBSA and MM/GBSA methods to estimate ligand-

binding affinities. Expert Opin Drug Discov. 2015;10(5):449-461. Doi: 10.1517/17460441.2015.1032936
35. Golovinskaia O, Wang C-K. The hypoglycemic potential of phenolics from functional foods and their mechanisms. Food Sci Hum Wellness. 2023;12(4):986-1007. Doi: 10.1016/j.fshw.2022.10.020
36. Zhou P, Li T, Zhao J, Al-Ansi W, Fan M, Qian H. Grain bound polyphenols: Molecular interactions, release characteristics, and regulation mechanisms of postprandial hyperglycemia. Food Res Int. 2025;208:116291. Doi: 10.1016/j.foodres.2025.116291
37. Gong L, Feng D, Wang T, Ren Y, Liu Y, Wang J. Inhibitors of *α*-amylase and *α*-glucosidase: Potential linkage for whole cereal foods on prevention of hyperglycemia. Food Sci Nutr. 2020;8(12):6320-6337. Doi: 10.1002/fsn3.1987
38. Wibowo S, Wardhani SK, Hidayati L, Wijayanti N, Matsuo K, Costa J. Investigation of α-glucosidase and α-amylase inhibition for antidiabetic potential of agarwood (*Aquilaria malaccensis*) leaves extract. Biocatal Agric Biotechnol. 2024;58:103152. Doi: 10.1016/j.bcab.2024.103152
39. Yilmazer-Musa M, Griffith AM, Michels AJ, Schneider E, Frei B. Grape seed and tea extracts and catechin 3-gallates are potent inhibitors of *α*-amylase and *α*-glucosidase activity. J Agric Food Chem. 2012;60(36):8924-8929. Doi: 10.1021/jf301147n
40. Ferenczy GG, Kellermayer M. Contribution of hydrophobic interactions to protein mechanical stability. Comput Struct Biotechnol J. 2022;20:1946-1956. Doi: 10.1016/j.csbj.2022.04.025
41. Patil R, Das S, Stanley A, Yadav L, Sudhakar A, Varma AK. Optimized hydrophobic interactions and hydrogen bonding at the target-ligand interface leads the pathways of drug-designing. PLoS One. 2010;5(8):e12029. Doi: 10.1371/journal.pone.0012029
42. Chi T, Wang M, Wang X, Yang K, Xie F, Liao Z. PPAR-γ Modulators as Current and Potential Cancer Treatments. Front Oncol. 2021;Volume 11 - 2021. Doi: 10.3389/fonc.2021.737776
43. Zhu Z, Guan Y, Gao S, Guo F, Liu D, Zhang H. Impact of natural compounds on peroxisome proliferator-activated receptor: Molecular effects and its importance as a novel therapeutic target for neurological disorders. European J Med Chem. 2025;283:117170. Doi: 10.1016/j.ejmech.2024.117170
44. Chaiya P, Senarat S, Phaechamud T, Narakornwit W. In vitro anti-inflammatory activity using thermally inhibiting protein denaturation of egg albumin and antimicrobial activities of some organic solvents. Mater Today: Proc. 2022;65:2290-2295. Doi: 10.1016/j.matpr.2022.04.916
45. Prasathkumar M, Raja K, Vasanth K, Khusro A, Sadhasivam S, Sahibzada MUK. Phytochemical screening and in vitro antibacterial, antioxidant, anti-inflammatory, anti-diabetic, and wound healing attributes of *Senna auriculata* (L.) Roxb. leaves. Arab J Chem. 2021;14(9):103345. Doi: 10.1016/j.arabjc.2021.103345
46. Cui J, Jia J. Natural COX-2 Inhibitors as Promising Anti-inflammatory Agents: An Update. Curr Med Chem. 2021;28(18):3622-3646. Doi: 10.2174/0929867327999200917150939
47. Ju Z, Li M, Xu J, Howell DC, Li Z, Chen FE. Recent development on COX-2 inhibitors as promising anti-inflammatory agents: The past 10 years. Acta Pharm Sin B. 2022;12(6):2790-2807. Doi: 10.1016/j.apsb.2022.01.002
48. Desai SJ, Prickril B, Rasooly A. Mechanisms of Phytonutrient Modulation of Cyclooxygenase-2 (COX-2) and Inflammation Related to Cancer. Nutr Cancer. 2018;70(3):350-375. Doi: 10.1080/01635581.2018.1446091
49. Chen W, Zhong Y, Feng N, Guo Z, Wang S, Xing D. New horizons in the roles and associations of COX-2 and novel natural inhibitors in cardiovascular diseases. Mol Med. 2021;27(1):123. Doi: 10.1186/s10020-021-00358-4
50. Ansari P, Reberio AD, Ansari NJ, Kumar S, Khan JT, Chowdhury S. Therapeutic Potential of Medicinal Plants and Their Phytoconstituents in Diabetes, Cancer, Infections, Cardiovascular Diseases, Inflammation and Gastrointestinal

Disorders. Biomedicines. 2025;13(2). Doi: 10.3390/biomedicines13020454

51. Kavya P, Theijeswini RC, Gayathri M. Phytochemical analysis, identification of bioactive compounds using GC-MS, in vitro and in silico hypoglycemic potential, *in vitro* antioxidant potential, and *in silico* ADME analysis of Chlorophytum comosum root and leaf. Front Chem. 2024;12:1458505. Doi: 10.3389/fchem.2024.1458505
52. Mahgoub S, Al-Awadi S, Abdelfatah H, Alshehry G, Alhassani WE, Alqurashi AF. GC–MS and HPLC analysis of bioactive compounds in Globe artichoke extract to enhance antioxidant and antibacterial properties in low-salt Domiati cheese. Appl Food Res. 2025;5(1):100800. Doi: 10.1016/j.afres.2025.100800